The Cost of Uncertainty
in Climate Tipping Points[*]

Andrea Titton[†]

October 22, 2024

Abstract

Climate tipping points introduce abrupt, irreversible shifts in the climate system, potentially locking the world into a high-temperature regime that is difficult, if not impossible, to reverse. This paper examines the economic consequences of such tipping points, focusing on the costs associated with their unpredictability and irreversibility. Using an integrated assessment model with a climate system exhibiting positive feedback, I compute optimal abatement policies under different assumptions about the proximity of tipping points. To bound the economic cost of uncertainty surrounding the exact location of the tipping point, I compare two scenarios: one where a "wishful thinker" planner assumes the tipping point is remote and delays abatement, and another where a "prudent" planner assumes incorrectly that the tipping point is imminent. This uncertainty can cost society up to 35% of current output. Furthermore, I show that in face of uncertainty, prudence, however costly,is cheaper than wishful thinking. Hence, when in doubt, abate.

As global temperatures rise due to greenhouse gas emissions from human activities, positive feedback mechanisms in the climate system can drive the world past critical thresholds, known as tipping points, into a regime of high temperatures. These tipping points pose a challenge when calculating optimal abatement strategies and, hence, developing policy tools like carbon budgets and the social cost of carbon, as society must balance the immediate economic benefits of emissions with the long-term climate damages they cause. First, tipping points cannot be predicted by just observing historical data (Ben-Yami et al., 2024), giving policymakers little time to react once they are detected. Second, as crossing a tipping point triggers a new possibly irreversible climate regime, climate damages suddenly increase. This discontinuity implies that evaluating optimal abatement policies using marginalist analysis, such as the social cost of carbon, can lead astray.

In this paper, I study the economic costs of unpredictable and irreversible climate tipping points. Using an integrated assessment model that incorporates positive feedback effects, I compute optimal abatement strategies under two different scenarios: one where a tipping point is imminent and another where it is remote. These scenarios are calibrated to reflect extreme cases from the climate literature (Armstrong McKay et al., 2022; Seaver Wang et al., 2023). I then quantify the upper bound of the economic losses through two experiments. The first measures the cost incurred by a "wishful thinker" social planner who mistakenly assumes the tipping point is remote, delaying optimal abatement until after it is crossed. This serves as an upper bound on the cost of under-abating. The second considers a "prudent" planner who incorrectly assumes the tipping point is imminent, leading to more aggressive abatement. This serves as an upper bound on the cost of over-abating. Together, these scenarios provide an upper bound on the economic costs of tipping, without requiring prior assumptions about the tipping point's exact location and avoiding marginalist calculations, which are ill-defined in the presence of tipping points. When compared with the optimal abatement strategies, these two scenarios give an estimate of

the cost of uncertainty: how much is society willing to pay to determine the tipping point and switch to an optimal abatement strategy.

I show that the cost of uncertainty in tipping points can be as large 26.25 trillions of US $ per year or 35 % of current world output. Reacting to this uncertainty by prudence and minimising the risk of tipping, requires quick abatement efforts, which incur in large adjustment costs. Reacting to this uncertainty by wishful thinking and delaying abatement, locks the world with high chance into a hot regime characterised by large climate damages. Both are very costly approaches, yet wishful thinking can cost up to 3.2 trillions of US $ per year more than prudence. Hence, when faced with uncertainty, for policymakers it is cheaper to tread with caution.

The rest of the paper is structured as follows. Section 1 puts the current paper in the context of the climate and environmental economic literature and highlights its contributions. Section 2 presents a stylised version of the model which displays the same qualitative feature: an unpredictable and irreversible tipping point. This simplified model serves as illustration of the major challenges faced in computing optimal abatement in the more general model. Section 3 introduces the climate model, the economy model, and the planner problem. Section 4 computes optimal abatement policies when tipping points are known. Section 5 introduces the "wishful thinking" and "prudent" social planner problem and computes the upper bounds on the economic cost of tipping points. Finally, section 6 draws policy implications and concludes.

1   Related Literature

A large recent literature in economics has highlighted the importance of correctly incorporating climate dynamics when analysing the economic trade-off between emissions and climate damaged we are currently facing. The key challenge is to develop integrated assessment models that, on the one hand, are sufficiently simple to be integrated into a dynamic optimisation problem, necessary to compute the economic costs of climate change and optimal abatement

policies, and, on the other hand, are able to reproduce the key dynamics of larger, more accurate climate models. Dietz et al. (2020) show, for example, how may climate models used in economics display unrealistic lags between emissions and temperature increase and that this yields insufficiently ambitious abatement policy recommendations. Another feature of the climate dynamic that has drawn a lot of attention in economics are climate tipping points (Li, Crépin and Lindahl, 2024). These are the focus of this paper.

Early work dealing with uncertain tipping points in environmental economics (Kamien and Schwartz, 1971; Nævdal and Oppenheimer, 2007; Tsur and Zemel, 1996, among others) has modelled tipping points via stochastic jump processes. At each moment in time either temperature or atmospheric carbon concentration experiences a discontinuous jump with some probability known to the planner. This approach was introduced in climate economics by Pindyck and Wang (2013), taken inspiration from the work on climate catastrophes by Barro (2009). It has been successfully employed in modelling climate tipping points by, for example, Lontzek et al. (2015), Cai, Lenton and Lontzek (2016), and Van Der Ploeg and De Zeeuw (2018). This has several advantages as it allows to readily incorporate ambiguity concerns (Lemoine and Traeger, 2016), learning (Lemoine and Traeger, 2014), and self exciting processes (Hambel, Kraft and Schwartz, 2021). Furthermore, it is analytically tractable and can be used to derive closed form approximations for the contribution of tipping points to the social cost of carbon (Li, Crépin and Lindahl, 2024; Van den Bremer and Van der Ploeg, 2021). Nevertheless, this modelling choice lacks two crucial features that are the focus of this paper. First, climate tipping points can introduce different temperature regimes. Barro style disasters are not suited to model these different regimes as they simply model single transient catastrophic events. Second, it requires to define a probability distribution on the tipping event, be that real or the belief of the social planner.

Another approach is to model feedbacks in the climate dynamics explicitly. This approach is closer to the real behaviour of the climate system (McGuffie

and Henderson-Sellers, 2014) and is the standard approach adopted in more complex climate modelling (e.g. Smith et al. 2017). Furthermore, optimisation over such systems has a long history in economics (Skiba, 1978) and has been developed extensively in environmental economics (Mäler, Xepapadeas and de Zeeuw, 2003; Wagener, 2013) and, specifically, in climate economics (Greiner and Semmler, 2005; Nordhaus, 2019; Wagener, 2015). This approach as one drawback: it requires one to make an assumption on how large the feedbacks are and when they kick in. These two facts are objects of contention (Armstrong McKay et al., 2022; Seaver Wang et al., 2023).

In this paper, I bridge these two approaches. By embedding and calibrating a positive climate feedback in a state of the art integrated assessment model (Hambel, Kraft and Schwartz, 2021), I obtain empirical estimates on the costs of uncertainty of tipping points. The focus of the two extreme scenarios, a "wishful thinker" and a "prudent" planner, allows to obtain upper bound on the cost of under-abating and suffering climate damages and over-abating and paying large adjustment costs. These serve then as an upper bound for the overall cost of tipping points. Despite being only upper bounds, these estimates do not require an arbitrary prior on the tipping point and can be computed in a scenario of multiple climate regime.

Finally, the numerical solver developed in the paper contributes to the literature on controlled stochastic processes by developing a parallelisation algorithm, based on Bierkens, Fearnhead and Roberts (2019), for the class of solver introduced in Kushner and Dupuis (2001), and extending their results to recursive utilities.

2 Stylised Example

Before turning to the full model, this section introduces a stylised integrated assessment model with a tipping point between multiple temperature regimes. The climate component of the model employs a stylised model of positive feedbacks, compared to the full model presented in section 3.1. In addition, the

planner objective is reduced to a simple optimal stopping problem. Despite this it illustrates the two main challenges tipping points introduce when computing optimal abatement. First, their unpredictability hinders evaluation of future damages. Second, their irreversibility makes analyses based on marginal emission benefits and marginal temperature damages incomplete.

Emissions of CO_2 from human economic activity E_t [$Gt\,CO_2$] raise CO_2 atmospheric concentration M_t [p.p.m.],

$$\frac{dM_t}{dt} = \xi_m E_t \tag{1}$$

where ξ_m converts $Gt\,CO_2$ to p.p.m.. As CO_2 is a greenhouse gas, an increase in its concentration M_t compared to pre-industrial levels M^p in turn, increases average temperature T_t [°C]. The change in temperature is given by

$$\frac{dT_t}{dt} = G_0 \log\left(\frac{M_t}{M^p}\right) - \lambda T_t, \tag{2}$$

where G_0 is the size of the greenhouse gas effect and λ is a stabilisation rate of temperature[1]. In this model, temperature tends towards the steady state

$$T_t \to \frac{G_0}{\lambda} \log\left(\frac{M_t}{M^p}\right) \quad \text{as } t \to \infty. \tag{3}$$

Hence, as carbon concentration rises, so does the steady state temperature. Suppose, for example, that emissions E_t are constant at some level $\bar{E}$, such that CO_2 concentration grows linearly $M_t = \bar{E}\,t + M^p$. In this case, average temperature T_t grows as illustrated in Figure 1. Consider now a social planner who derives utility $u(E_t)$ from CO_2 emissions E_t and disutility $d(T_t)$ from temperature T_t, and discounts both at a rate ρ. For simplicity assume the emissions are constant at a level $\bar{E}$ and the social planner needs to decide at what time τ society ought to stop emitting. At that point society loses the benefits of emissions $u(\bar{E})$ and pays the damages of the resulting temperature $d(T_\tau)$. To summarise, the plan-

---

[1]Throughout this section, I assume for illustration purposes $G_0 = 1$, $\xi_m = 1$, and $\lambda = 1$.
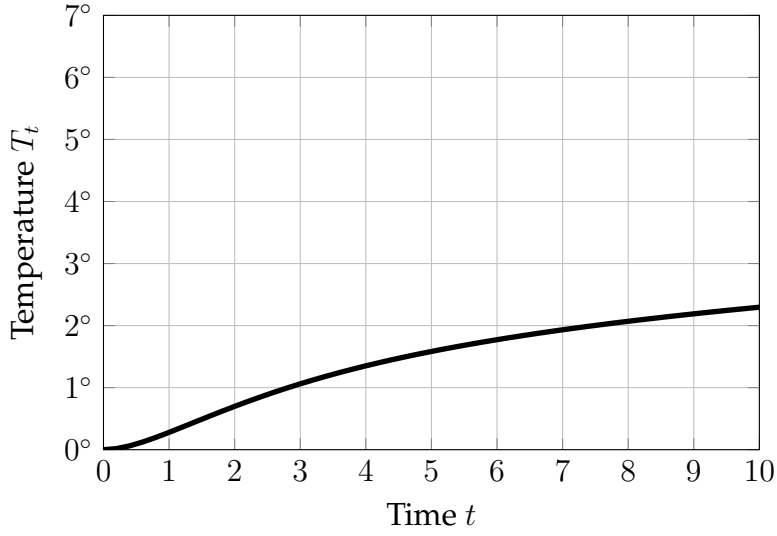
Figure 1: Path of temperatures given by (2), assuming constant emissions $E_t = \bar{E}$.

ner is trying to maximise

$$J(\tau) := (1 - e^{-\rho\tau})\, u(\bar{E}) - e^{-\rho\tau}\, d(T_\tau) \tag{4}$$

by choosing an emission stopping time $\tau \geq 0$. This problem is readily solved by a marginalist planner: the optimal time τ to stop emissions is when an additional instant utility of emission does not justify the marginal increase in temperature damages, or $\partial J / \partial \tau = 0$.

Yet, unlike the model in equation (2), the climate system is highly complex. One such complexity arises due to positive temperature feedbacks, such as ice melting which reduces the earth's albedo or water evaporating and acting as a greenhouse gas. One way to introduce these in the toy model presented here is to assume the stabilisation rate λ to be a function of average temperature T_t[2]. In

---

[2] For illustration purposes, in this section I assume

$$\lambda(T_t) = aT_t^2 - 3\sqrt{\frac{c}{a}}T + 2c \tag{5}$$

where $c = 1/2$ is a scale parameter and $a = 0.08$ denotes the intensity of the feedback. Any $\lambda(T_t)$ increasing in T_t would display the same multiplicity of equilibria.

this case, the change in temperature (2) is given by

$$\frac{\mathrm{d}T_t}{\mathrm{d}t} = G_0 \log\left(\frac{M_t}{M^p}\right) - \lambda(T_t)\, T_t. \tag{6}$$

Figure 2 shows the change in temperature $\frac{\mathrm{d}T_t}{\mathrm{d}t}$ (6) as a function of temperature T_t for carbon concentration at the pre-industrial level (left panel), 50% larger (middle panel) and twice as large (right panel). As in the model without feed-
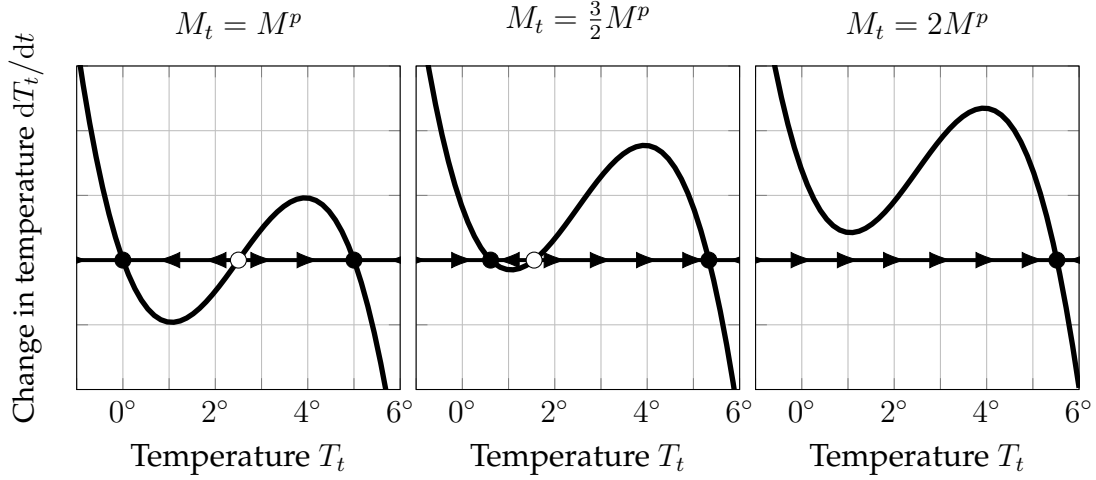

Figure 2: Change in temperature over time $\frac{\mathrm{d}T_t}{\mathrm{d}t}$ as a function of temperature T_t for three levels of atmospheric carbon concentration. The marker represents the steady state and the arrows indicate whether temperature is increasing (right) or decreasing (left).

backs (2), if carbon concentration is at its pre-industrial level (left panel) there is stable level of temperature at $T_t = 0$ (left black marker). In addition to this, a new stable high temperature equilibrium is formed (right black marker). In this equilibrium, the positive feedback has trapped temperature into a high regime, for example, if all ice caps have melted the surface albedo is sufficiently low that ice is unable to form again. As carbon concentration increases (from left to right panel), the average temperature raises. Yet, unlike in the case of no feedback, the system goes through a tipping point[3]: the low temperature equilibrium becoming unfeasible triggers a sudden rise in temperature as it converges to the higher equilibrium. This phenomenon poses two problems from the point of view of the social planner trying to evaluate the trade-off between current

---

[3]The system undergoes a saddle-node bifurcation.

emissions and future climate damages. First, if the temperature dynamics (6) are uncertain, one cannot hope to learn them from simply observing the path of temperature (Ben-Yami et al., 2024). To illustrate this, Figure 2 shows the path of temperature under constnat emissions in the presence of feedback (solid line) and in the linear case (dashed line). The two trajectories are extremely close, until the tipping point is reached. After this, they rapidly diverge. Second,
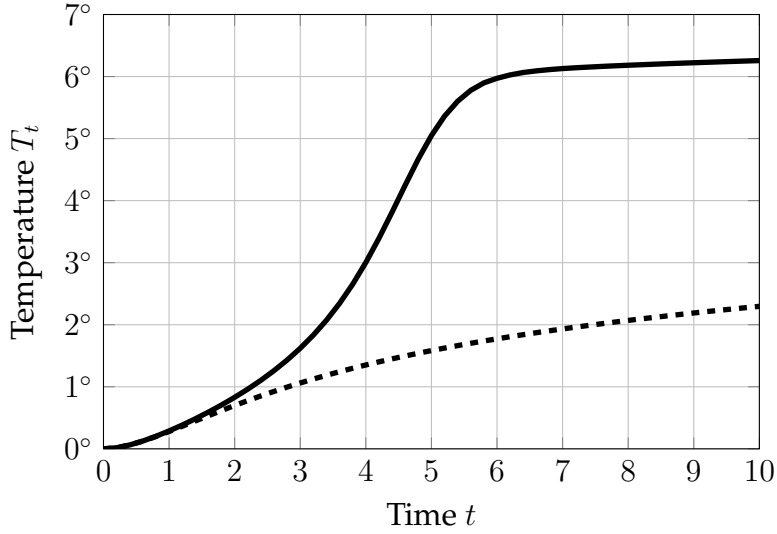

Figure 3: Path of temperatures given by (6), assuming constant emissions $E_t = \bar{E}$. The dashed line is the path without feedback as in Figure 1

marginalist calculations are not sufficient to solve the emission stopping problem given in equation (4). Figure 4 shows the objective function J as a function of the stopping time. In a low temperature regime, delaying abating emissions is always optimal, as the marginal benefits of emissions are always greater than the marginal climate damages. This brings the climate ever closer to the tipping point. At that point, there is no such thing as marginal damages as any small increase in emission can push the climate into a high temperature regime. The costs of tipping are hence not internalised in the marginal $\partial J/\partial \tau$. Hence, basing policies on the marginal damages of delaying abatement for slightly longer can move one arbitrarily close to tipping.
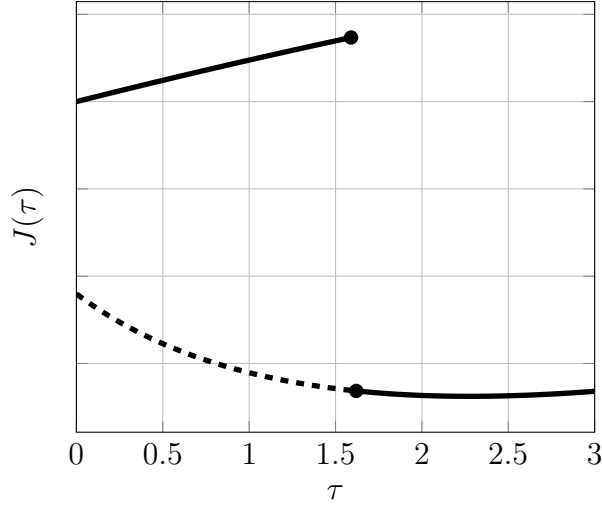
Figure 4: Objective J as a function of stopping time τ (4).

3 Model

The following extends the stylised model from section 2. First, section 3.1.1 introduces carbon sinks and their interaction with atmospheric carbon concentration. Then, section 3.1.2 presents the temperature dynamics and the positive feedback. Section 3.1.3 discusses the resulting tipping points in the climate system. Finally, section 3.2 presents the Harrod–Domar economy.

As in the stylised model above, the positive feedbacks in the climate dynamics introduce a tipping point. Yet, its added realism allows us to calibrate it and to produce meaningful estimates on the costs of such tipping points. The model and the calibration extend that of Hambel, Kraft and Schwartz (2021). The calibration of both the climate model and the economy is updated to the year 2020.

3.1 Climate Model

3.1.1 CO_2 concentration and carbon sinks

Emissions from human economic activity E_t increase the average atmospheric concentration of CO_2 M_t. This, in turn, decays into natural sinks N_t. The rate of decay $\delta_m(N_t)$ falls in the quantity of carbon dioxide already stored in the natural

sinks N_t, as the sinks saturate (Le Quéré et al., 2007; Shi et al., 2021). Hence, this evolves as

$$\xi_m \, \mathrm{d}N_t = \delta_m(N_t)M_t \ \mathrm{d}t \tag{7}$$

where ξ_m converts $\mathrm{Gt}\,\mathrm{CO}_2$ to $\mathrm{p.p.m.}$.

To focus on abatement efforts I rewrite variables in deviation from a business-as-usual scenario scenario. This scenario is calibrated using the IPCC SPSS5 projections (Kriegler et al., 2017). Denote by E_t^b the emissions under such scenario, and by M_t^b and N_t^b the resulting carbon in the atmosphere and in natural sinks, respectively. The atmospheric concentration M_t^b under business as usual emissions evolves as

$$\frac{\mathrm{d}M_t^b}{M_t^b} = \gamma_t^b \, \mathrm{d}t + \sigma_m \, \mathrm{d}W_{m,t} \tag{8}$$

where

$$\gamma_t^b := \xi_m \frac{E_t^b}{M_t^b} - \delta_m(N_t^b) \tag{9}$$

and $W_{m,t}$ is a Wiener process. This scenario describes an energy intensive future, in which fossil fuel usage develops rapidly and little to no abatement takes place. Using this scenario, I then calibrate the implied growth rate of carbon concentration γ_t^b. Figure 5 shows the results of the calibration (Appendix C). The left figure shows the path of the business as usual growth rate γ_t^b and the
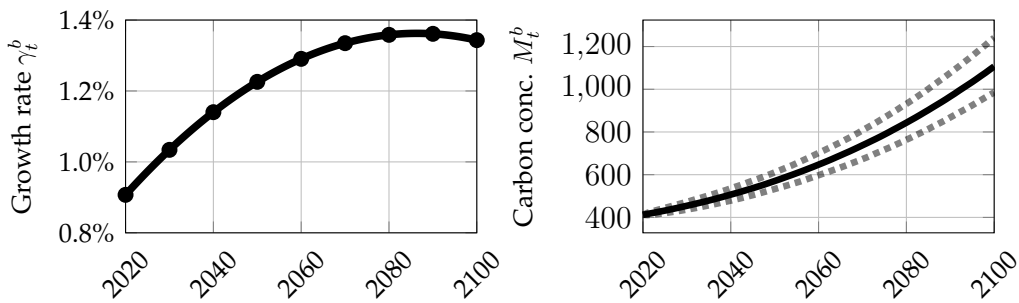

Figure 5: Growth rate of carbon concentration in the business as usual scenario γ_t^b and median path (solid) of business as usual carbon concentration M_t^b (8) with 95% simulation interval (dashed).

right figure shows the resulting growth of carbon concentration M_t^b. The carbon concentration in this scenario is assumed to grow at an increasingly fast rate until 2080, when the growth rate peaks just below 1.4%. Thereafter, the

growth rate starts declining. The growth rate of carbon concentration γ_t^b is always positive, hence in the business as usual scenario, carbon concentration is always increasing.

Abatement efforts α_t lower the growth rate of carbon concentration M_t vis-à-vis the business as usual scenario M_t^b. That is, the growth rate of carbon concentration M_t satisfies

$$\frac{\mathrm{d}M_t}{M_t} = \left(\gamma_t^b - \alpha_t\right)\mathrm{d}t + \sigma_m\,\mathrm{d}W_{m,t} \tag{10}$$

where $\mathrm{d}W_{m,t}$ is a Wiener process.

Not implementing any abatement policy $\alpha_t = 0$ corresponds to a business as usual scenario $M_t \equiv M_t^b$, while implementing a full abatement policy $\alpha_t = \gamma_t^b$ stabilises carbon concentration. Any abatement policy α_t can be implicitly linked back to the corresponding level of emissions by introducing an emission reduction rate $\varepsilon(\alpha_t)$, which keeps tracks of what percentage of emission has been abated

$$E_t = \left(1 - \varepsilon(\alpha_t)\right)E_t^b. \tag{11}$$

In this paper I assume that the planner does not have access to carbon capture technology. This is implemented by imposing that abatement cannot exceed the growth rate of carbon concentration and the carbon decay into natural sinks, namely

$$\alpha_t \leq \gamma_t^b + \delta_m(N_t). \tag{12}$$

3.1.2 Temperature

Earth's radiating balance, in its simplest form, prescribes that an equilibrium temperature $\bar{T}$ is determined by equating incoming solar radiation S with outgoing long-wave radiations $\eta\sigma\bar{T}^4$, where σ is the Stefan-Boltzmann constant and η is an emissivity rate. Due to the presence of greenhouse gasses, certain wavelengths are scattered and, hence, not emitted[4]. This introduces an addi-

---

[4]See Ghil and Childress (2012) for a more detailed discussion.

tional radiative forcing G which yields the balance equation $S = \eta\sigma\bar{T}^4 - G$. Focusing on the role of increased CO_2, as opposed to other greenhouse gases, we can decompose the greenhouse radiative forcing term G into a constant component G_0 and a component which depends on the steady state level of CO_2 concentration in the atmosphere M_t with respect to the pre-industrial level M^p, such that

$$G \equiv G_0 + G_1 \log(M_t/M^p). \tag{13}$$

I introduce a feedback in the temperature by assuming that the absorbed incoming solar radiation is increasing in temperature. This choice can be seen as a stylised model of the ice-albedo feedback (Ashwin et al., 2012; McGuffie and Henderson-Sellers, 2014), yet, any positive feedback in temperature dynamics yields a similar interpretation. Similarly, incoming solar radiation S can be decomposed as $S_0 \left(1 - \lambda(T_t)\right)$ where the function $\lambda(T_t)$ transitions from a higher λ_1 to a lower level $\lambda_1 - \Delta\lambda$ via a smooth transition function $L(T_t)$. To control at which level of temperature the transition occurs the transition functions take the form

$$\lambda(T_t) := \lambda_1 - \Delta\lambda\big(1 - L(T_t)\big) \text{ with} \tag{14a}$$

$$L(T_t) := \frac{1}{1 + \exp\left(-L_1\left(T_t - T^c\right)\right)} \tag{14b}$$

where T^c is the level of temperature at which the feedback effect begins and L_1 is a speed parameter.

The costs that society incurs if it behaves under the wrong assumption over T^c are the focus of the subsequent sections. Best estimates from climate sciences are that many such transitions occur for average global temperatures between $1.5°$ and $3°$ over pre-industrial levels (Seaver Wang et al., 2023). A large body of literature has focused on estimating critical thresholds associated with climate tipping (e.g. Boulton, Allison and Lenton 2014; Van Westen, Kliphuis and Dijkstra 2024), yet for many such tipping points either the uncertainty is too large (Ben-Yami et al., 2024) or it is not theoretically possible to do so (Ditlevsen

and Johnsen, 2010; Wagener, 2013). To avoid attaching an arbitrary prior over such threshold, in this paper I choose to focus on two extreme scenarios: one in which the tipping point is *imminent* $T^c = 1.5°$ and one in which it is *remote* $T^c = 2.5°$. The parameter $\Delta\lambda$ is calibrated by matching the climate sensitivity, that is, the expected equilibrium temperature of doubling CO_2 concentration $M_t = 2M^p$, of $4.5°$, which is the upper end of the range deemed very likely in AR6 (IPCC, 2023). Figure 6 shows the transition function (14) under these two scenarios. Despite being a highly stylised and reduced form representation of
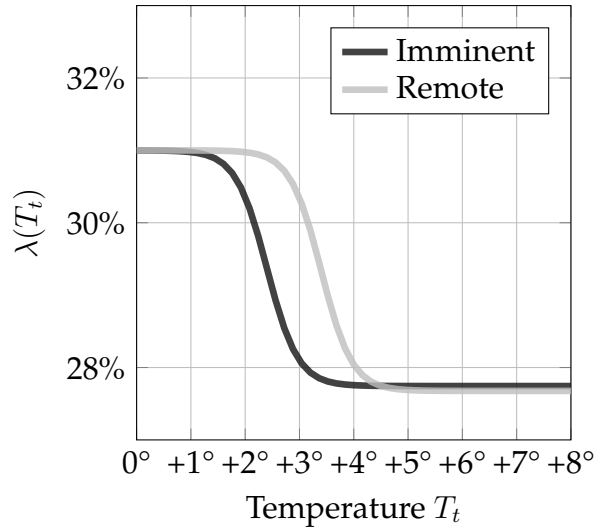

Figure 6: Coefficient $\lambda(T)$ for different threshold temperatures $T^c \in \{1.5, 3.5\}$

a complex and spatially heterogeneous process, λ captures the core mechanism behind feedback processes in the temperature dynamics that can generate tipping points (McGuffie and Henderson-Sellers, 2014). These simple feedback dynamics allow us to discuss and estimate the costs of ending in a new regime, what ought to be done to prevent this from happening or not, and the regret associated with their uncertainty.

Putting these processes together we can write the two determinants of temperature dynamics: radiative forcing, which only depends on temperature,

$$r(T_t) \coloneqq S_0 \left(1 - \lambda(T_t)\right) - \eta\sigma T_t^4 \tag{15}$$

and the greenhouse gas effect, which only depends on atmospheric carbon con-

centration

$$g(M_t) := G_0 + G_1 \log(M_t/M^p). \tag{16}$$

Under these two drivers, temperature changes are given by

$$\epsilon \, dT_t = r(T_t) \, dt + g(M_t) \, dt + \sigma_T \, dW_{T,t}, \tag{17}$$

where ϵ is the thermal inertia and $W_{T,t}$ is a Wiener process.

3.1.3 Tipping Points

The presence of the feedback effect λ introduces tipping points in the temperature dynamics. This is illustrated in Figure 7. For a given level of carbon concentration $\bar{M}$, the temperature $\bar{T}$ tends towards radiative balance $r(\bar{T}) = -g(\bar{M})$ (solid line). For low values of carbon concentration $\bar{M} \lesssim 350$, such steady
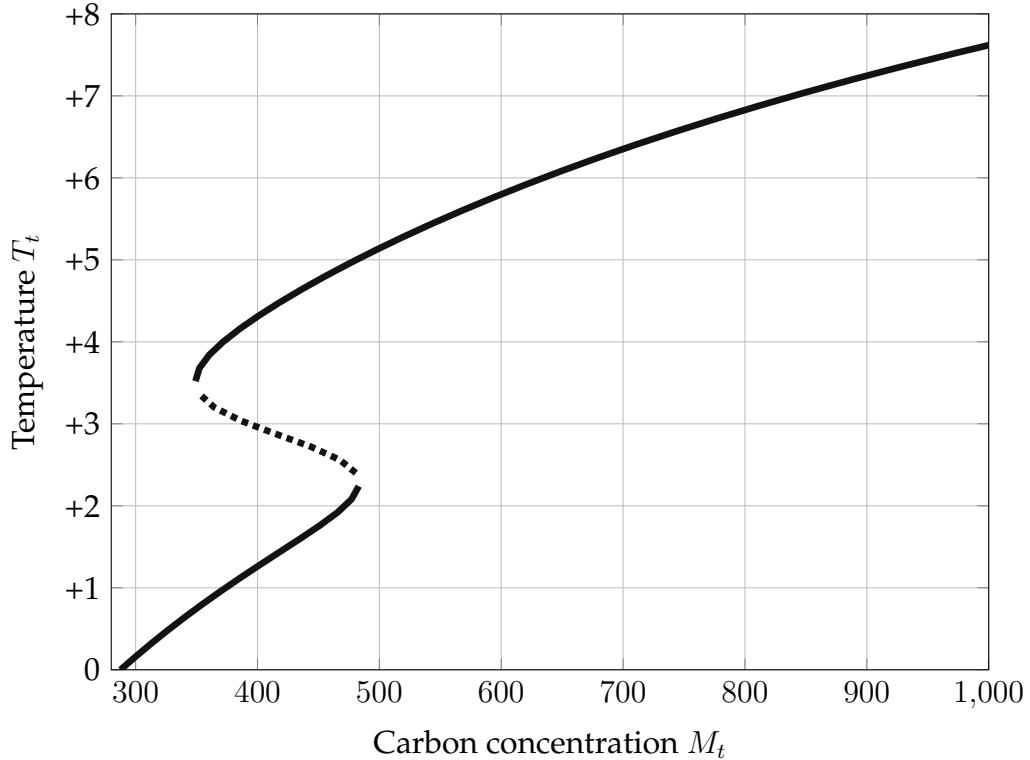

Figure 7: Steady states of temperature T_t and carbon concentration M_t for $T^c = 2°$. The solid and dashed lines represent attracting and repelling steady states, respectively.

state is unique. As more carbon dioxide gets added to the atmosphere, two

additional steady state levels of temperature $\bar{T}$ arise, one stable (upper solid line) and one separating unstable (dashed line). The presence of the additional steady state is hard to detect as the relationship between temperature T_t and carbon concentration M_t remains approximately log-linear. This makes estimating the presence of a tipping point and its threshold T^c unfeasible using purely historical data. As carbon concentration increases further $M_t \gtrsim 490$ and temperature crosses the critical threshold T^c, the old stable and low temperature regime is no longer feasible and only a high stable temperature regime remains. Any increase of carbon concentration at this tipping point then leads to a rapid increase in temperature to a this new steady state. Crucially, to revert the system back to the lower temperature regime, it is not sufficient to remove just the carbon that caused the system to tip, but society would have to remove all carbon until the only stable steady state is the low temperature, hence back to $M_t \lesssim 350$ ("walking along" the upper solid line). In the context of the example of an ice-albedo tipping point, at low level of carbon concentration the Earth's ice coverage is large and the albedo coefficient, that is, the percentage of solar radiation reflected by the lighter coloured surface. As temperature rises, and ice melts, the albedo decreases, which further contributes to temperature increases. This positive feedback might push the world into an "ice-free" regime with low albedo. To restore ice coverage temperature must decrease further than the increase of the tipping point.

Figure 8 displays how this mechanism impacts the dynamics of temperature under the business as usual scenario for an imminent tipping point, $T^c = 1.5°$ (darker), and a remote one, $T^c = 2.5°$ (lighter). The lines with the markers show a simulation of temperature T_t (17) and carbon concentration M_t under business as usual (8). Markers denotes the temperature and carbon concentration every 10 years starting from 2020. For the first two decades, the temperature dynamics are identical. Then, if the tipping point is imminent $T^c = 1.5°$, suddenly temperature grows rapidly to the new steady state and the system converges to a higher temperature regime, before the log-linear relationship

between temperature T_t and carbon concentration M_t is established again. This occurs much later whenever the critical temperature T^c is higher and, hence, the tipping point is remote.
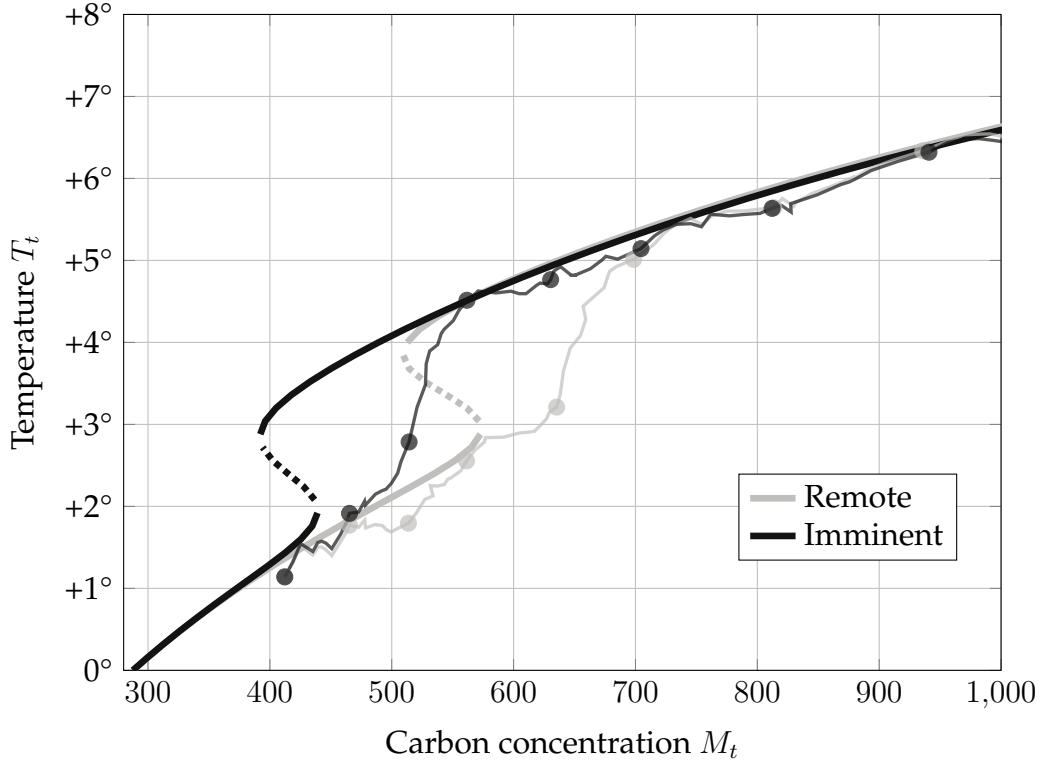

Figure 8: Steady states of temperature T_t and carbon concentration M_t for $T^c = 1.5°$ (dark) and $T^c = 2.5°$ (light). The solid and dashed lines represent attracting and repelling steady states, respectively. The marked line show two simulation of temperature and carbon concentration under the business as usual scenario. Markers denotes the temperature and carbon concentration every 10 years starting from 2020.

3.1.4 Irreversable Regime Changes against State-Distribued Catastrophes

Before turning to the economic model, in the following I illustrate the key differences between the modelling of tipping points in this paper and that of the previous literature in climate economics. This has, in large part, modelled tipping points by assuming that, at each moment in time, with some instantaneous probabilities $\pi(T_t)$ there is a temperature shock of size $q(T_t)$, both of which are increasing in temperature (e.g. Hambel, Kraft and Schwartz 2021; Lemoine and Traeger 2016; Van Der Ploeg and De Zeeuw 2018). This approach is also known as state-distributed catastrophe (Li, Crépin and Lindahl, 2024) and can

be traced back to Barro (2009) and Pindyck and Wang (2013). Formally, under this assumption, equation (17) of the climate model presented here becomes

$$\epsilon \, \mathrm{d}T_t = r_l(T_t) \, \mathrm{d}t + g(M_t) \, \mathrm{d}t + \sigma_T \, \mathrm{d}W_{T,t} + q(T_t) \, \mathrm{d}J_t(T_t) \tag{18}$$

where J_t is a Poisson process with arrival rate $\pi(T_t)$ and r_l, unlike r (15), is linear. As comparison, Figure 9 shows the distribution of temperature generated by the model of this paper (17) and the state-distributed catastrophe model (18), as calibrated in Hambel, Kraft and Schwartz (2021) (see Appendix D for more details on this calibration). Both models capture a key feature of tipping points:
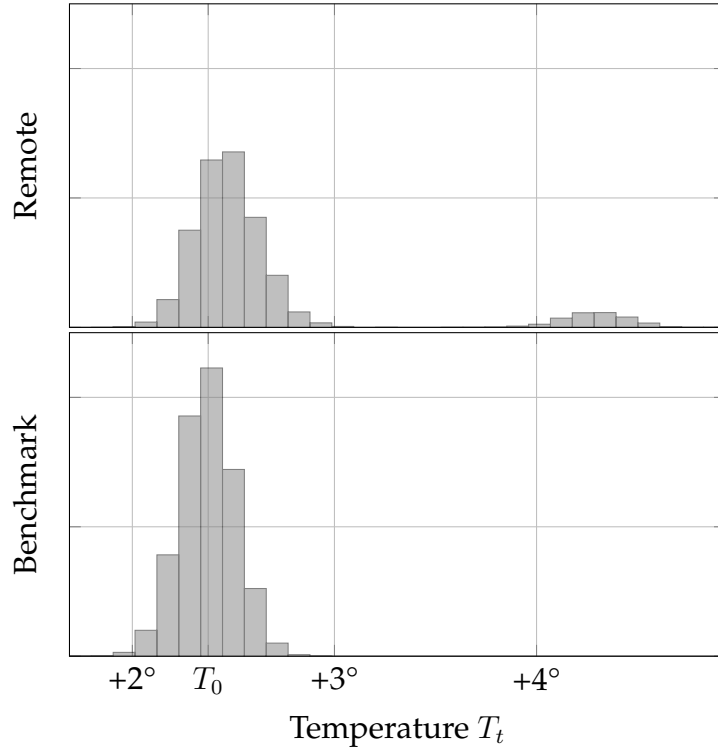

Figure 9: Distribution of temperature T_t obtained from simulation dT_t from (17) and (18) (benchmark) for 1000 years at a constant carbon concentration level $M = 540$ p.p.m. starting at T_0.

as carbon concentration rises, we expect warmer shocks to be more persistent and hence the steady state temperature distribution to be skewed (IPCC, 2023; Weitzman, 2014). Yet, the benchmark model does not display multiple temperature regimes. It is hence not suited to answer questions on the costs of irreversible tipping points. The climate model presented here (17) generates

multiple temperature regimes while producing skewed steady state temperature distributions.

3.2 Economy

In the following, the Harrod–Domar economy is introduced.

3.2.1 Capital Accumulation and Climate Damages

Output

$$Y_t = A_t K_t. \tag{19}$$

is the product of the capital stock K_t and its productivity A_t. The latter grows at a constant rate ϱ. Output Y_t can be used for investment in capital I_t, abatement expenditures B_t, or consumption C_t. This implies the nominal budget constraint

$$Y_t = I_t + B_t + C_t. \tag{20}$$

Capital K_t depreciates at a rate δ_k but can be substituted by capital investments I_t, which incurs, along with abatement expenditure B_t, in quadratic adjustment costs

$$\frac{\kappa}{2} \left(\frac{I_t + B_t}{K_t} \right)^2 K_t. \tag{21}$$

Climate change interacts with the economy by lowering capital growth via damages $d(T_t)$ which are increasing in temperature T_t. Following Weitzman (2012), I assume the damage function to take the form

$$d(T_t) := \xi\, T_t^v. \tag{22}$$

The calibrated damage function is displayed in Figure 10. This stylised form captures the empirical evidence that under higher temperature levels some forms of capital, particularly in the agricultural (Dietz and Lanz, 2019) or manufacturing sectors (Dell, Jones and Olken, 2009, 2012), become more expensive or harder to substitute. A common alternative in the literature is to assume that
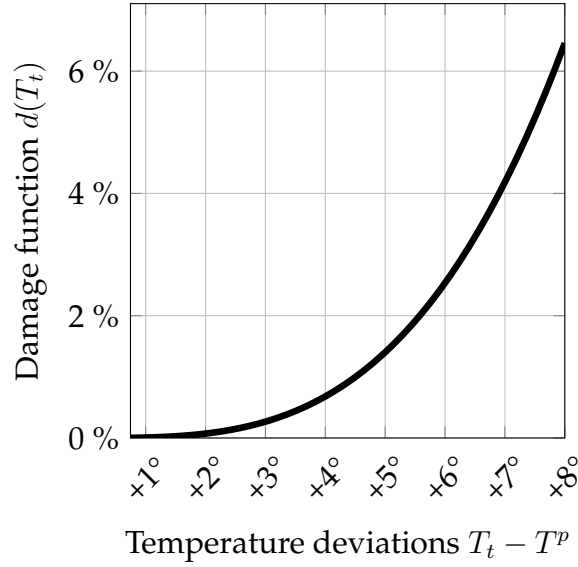
Figure 10: Damage function with the Weitzman (2012) calibration.

higher temperatures wipe out part of the capital stocks (Nordhaus, 1992). The comparison between these two assumption is carried out in Appendix **??** and a thorough treatment can be found in Hambel, Kraft and Schwartz (2021).

Combining the endogenous growth of capital and the climate damages, the growth rate of capital satisfies

$$\frac{\mathrm{d}K_t}{K_t} = \left(\frac{I_t}{K_t} - \delta_k - \frac{\kappa}{2} \left(\frac{I_t + B_t}{K_t} \right)^2 \right) \mathrm{d}t - d(T_t)\,\mathrm{d}t + \sigma_k\,\mathrm{d}W_k\,, \qquad (23)$$

where W_k is a Wiener process.

In the following, I link the abatement costs B_t with the abatement rate α_t, introduced in the previous section. Introduce $\beta_t := B_t/Y_t$ the fraction of output devoted to abatement. I assume this to be quadratic function of the fraction of abated emissions $\varepsilon(\alpha_t)$ (11), namely,

$$\beta_t(\varepsilon(\alpha_t)) = \frac{\omega_t}{2}\,\varepsilon(\alpha_t)^2. \qquad (24)$$

Under this assumption, no abatement is free, as $\beta_t(0) = 0$. At a fixed time t, an higher abatement rate α_t and hence an higher emission reduction $\varepsilon(\alpha_t)$ vis-à-vis the business as usual scenario, becomes increasingly costly at linear rate

$\omega_t \varepsilon(\alpha_t)$. It is common in the literature to assume the marginal abatement costs to be proportional to output and linear in abatement efforts (Baker, Clarke and Shittu, 2008; Dietz and Venmans, 2019; Nordhaus, 1992, 2017). As noted by Dietz and Venmans (2019, p.112-113), the proportionality with output arises because higher output growth increases energy demand. This must be satisfied with low-carbon energy technology which display decreasing marginal productivity. The linearity in abatement efforts is assumed as it matches the empirical estimates provided in the IPCC Fifth Assessment Report (2023).

As time progresses, so does abatement technology and a given abatement objective becomes cheaper, as a fraction of output. This is modelled by letting the exogenous technological parameter ω_t decrease exponentially over time

$$\omega_t = \omega_0 e^{-\omega_r t}. \tag{25}$$

Following (Nordhaus, 2017), I assume that full abatement $\varepsilon(\alpha_t) = 1$ costs 11% of GDP in 2020 and 2.7% of GDP in 2100. These estimates are in line with a large literature estimating marginal abatement curves (see the meta-analysis by Kuik, Brander and Tol 2009). The resulting marginal abatement curves are displayed in Figure 11.
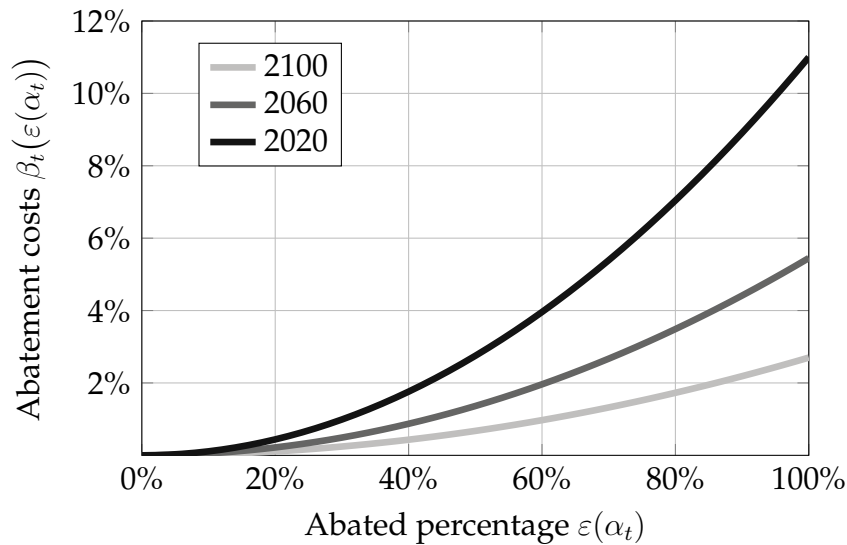

Figure 11: Calibrated marginal abatement curves $\beta'_t(\varepsilon) = \omega_t \varepsilon$ at different times t.

Finally, let

$$\chi_t := \frac{C_t}{Y_t} \tag{26}$$

be the fraction of output devoted to consumption. Using the budget constraint (20) and the two controlled rates, the abatement efforts α_t and the consumption rate χ_t, the growth rate of capital (23) can be rewritten as

$$\frac{\mathrm{d}K_t}{K_t} = \Big(\phi_t(\chi_t) - A_t \beta_t(\varepsilon(\alpha_t)) - d(T_t) \Big) \mathrm{d}t + \sigma_k \, \mathrm{d}W_{k,t} \tag{27}$$

where

$$\phi_t(\chi_t) := A_t(1 - \chi_t) - \frac{\kappa}{2} A_t^2 (1 - \chi_t)^2 - \delta_k \tag{28}$$

is an endogenous growth component, $\beta_t(\varepsilon(\alpha_t))$ is the fraction of output allocated to abatement for an abatement rate α_t, and $d(T_t)$ are the damages from climate change. This formulation makes the trade-off between climate abatement and economic growth apparent. Devoting fewer resources to abatement to pursue higher capital growth, and hence, output growth, yields higher future temperature and can put the economy in a lower growth path altogether.

Finally, as output Y_t is the product of capital K_t and productivity A_t, its growth rate differs from that of capital by the growth rate of productivity

$$\frac{\mathrm{d}Y_t}{Y_t} = \varrho + \frac{\mathrm{d}K_t}{K_t}. \tag{29}$$

4 Optimal Abatement

Given the climate and economic dynamics described in the previous section, in the following I introduce the objective of the social planner and the resulting maximisation problem. At time t given the state of temperature, carbon concentration, carbon in sinks, and output $X_t := (T_t, M_t, N_t, Y_t)$, societal utility is recursively defined as

$$V_t(X_t) = \sup_{\chi,\alpha} \mathbb{E}_t \int_t^\infty f(\chi_s(X_s)Y_s, V_s(X_s)) \, \mathrm{d}s \tag{30}$$

where χ and α are continuous policies over time and the state space, and f is the Epstein-Zin aggregator

$$f(C, V) := \rho \frac{(1-\theta) V}{1 - 1/\psi} \left(\left(\frac{C}{((1-\theta)V)^{\frac{1}{1-\theta}}} \right)^{1-1/\psi} - 1 \right). \qquad (31)$$

Consumption is integrated into a utility index by means of the Epstein-Zin integrator (Duffie and Epstein, 1992). This aggregator plays a dual role. First, it allows to disentangle the role of relative risk aversion θ, elasticity of intertemporal substitution ψ, and the discount rate ρ in determining optimal abatement paths. Second, it circumvents the known paradoxical result that abatement policies becomes less ambitious as society becomes more risk averse (Pindyck and Wang, 2013). As in Hambel, Kraft and Schwartz (2021), the model presented here assumes $\rho = 1.5\%$, $\theta = 10$ and $\psi = 0.75$. For a more detailed discussion on the calibration of these parameters see (Pindyck and Wang, 2013, Section 2) and for their role in determining optimal abatement see Hambel, Kraft and Schwartz (2021). Details on the numerical solution of problem (30) are given in Appendix A.

As mentioned above, we consider two possible dynamics for temperature T_t. One with an imminent and one with a remote tipping point. Let $\underline{\alpha}_t$ and $\overline{\alpha}_t$ be the optimal abatement in case of an imminent and a remote tipping point respectively. Figure 12 shows how optimal policies behaves in a regime with tipping points. Each panel shows the fraction of abated emissions ε_t compared to the business as usual in the imminent (left) and remote (right) tipping point, as a function of the current carbon concentration M_t. As the tipping point generates multiple temperature regimes for a given carbon concentration level M_t, each panel shows two curves. The lighter curve represents the optimal abatement before tipping, in a low temperature regime. The darker curve represents the optimal abatement after tipping, in a high temperature regime. The optimal policy is hence not unique and switches in the event of tipping. In case of an imminent tipping point (left panel) before having tipped (lighter curve),
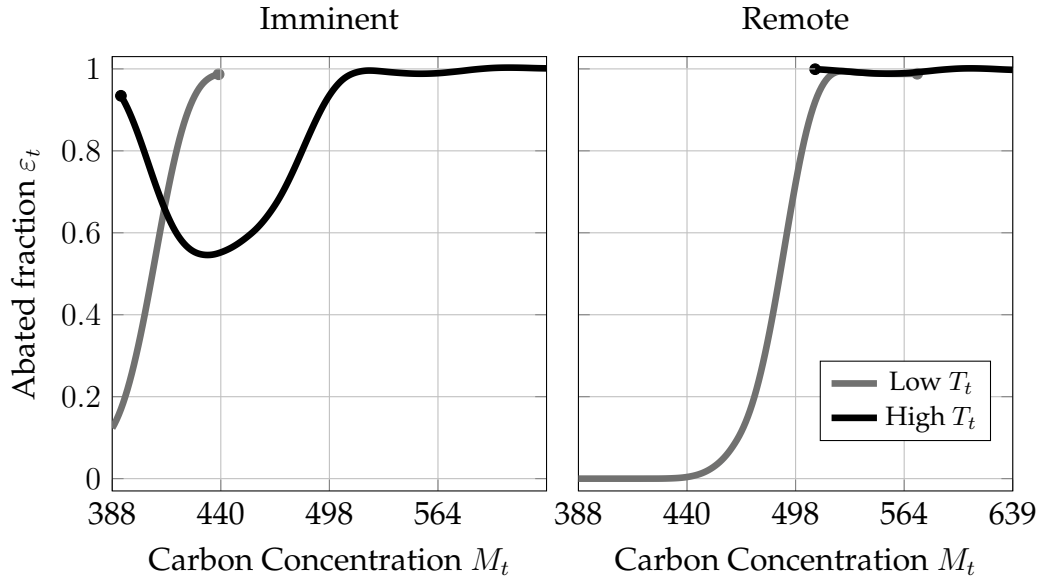
Figure 12: Fraction of abated emissions ε_t at different levels of carbon concentration M_t, for an imminent (left panel) and remote (right panel) point. To aid illustration, all other dimensions (T_t, N_t, Y_t) are set to their steady state value. As for some values of M_t there are two steady states of temperature T_t, two curves are shown.

the fraction of abated emission ε_t increases rapidly to 1 as carbon concentration rises. If the tipping point is crossed and the climate system switches to a high temperature regime abatement efforts are scaled back (darker curve) as the climate is irreversibly in a regime of high temperature. This results underpins a strong policy result: crossing a tipping point immediately weakens abatement incentives, hence, it is optimal to rapidly scale up abatement before that happens. This aspect of optimal abatement policies with tipping points cannot be captured by the social cost of carbon, since the marginal benefit of abating falls jumps down once the climate has tipped. Finally, notice that, if the climate has tipped but carbon concentration is low, it is still worth abating a large fraction of emissions (dark curve is u-shaped) because if carbon concentration is low a random negative shock in temperature can push the system back to a low-temperature regime, hence it is worth investing to delay the growth of carbon concentration. At the other extreme, if the tipping point is remote (right panel) it does not affect optimal policy. Abatement efforts are increasing in carbon concentration and full abatement is reached, in both regimes, at around 500 p.p.m.. In this case, direct climate damages are sufficiently large to warrant reaching

24

net-zero before there is any risk of a crossing the tipping point.

These policies, when implemented, yield a path of temperature and, as a consequence, temperature damages. Figure 13 shows the median path of the abated fraction of emission ε_t (solid line) and the resulting temperature path T_t with 95% simulation intervals (dotted lines), for an imminent (left panel) and a remote (right panel) tipping point.
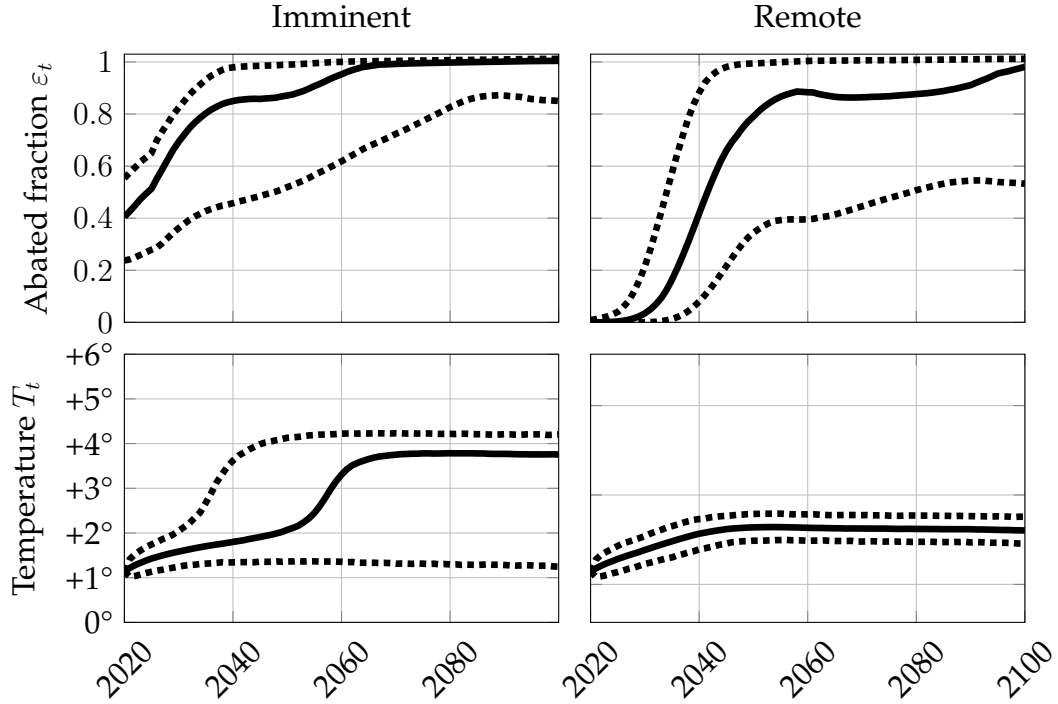

Figure 13: Median (solid line) and 95% simulation intervals (dotted line) of abated fraction ε_t and temperature T_t under optimal policies in the imminent and remote scenarios. 10000 simulations.

As expected, in case of an imminent tipping point, abatement is promptly ramped up. In the median case 40 % of the business-as-usual emissions are abated immediately. Thereafter, abatement ramps up and net-zero is attained by 2060. These large efforts are not sufficient to completely prevent tipping as by 2040 the climate system has tipped with 5% probability and by 2060 with 50% probability. In case the tipping point is remote, the planner has more time to postpone abatement, which is cheaper in the future, and is able to stabilise temperature at around 2° without tipping. When choosing an abatement policies, the planners are balancing two sources of societal costs: abatement expenditures $\beta_t(\epsilon_t)$

and their adjustment costs against climate damages $d(T_t)$. Figure 14 shows the average costs in each decade, as a fraction of output Y_t, in the median scenario, broken down into these three cost sources.
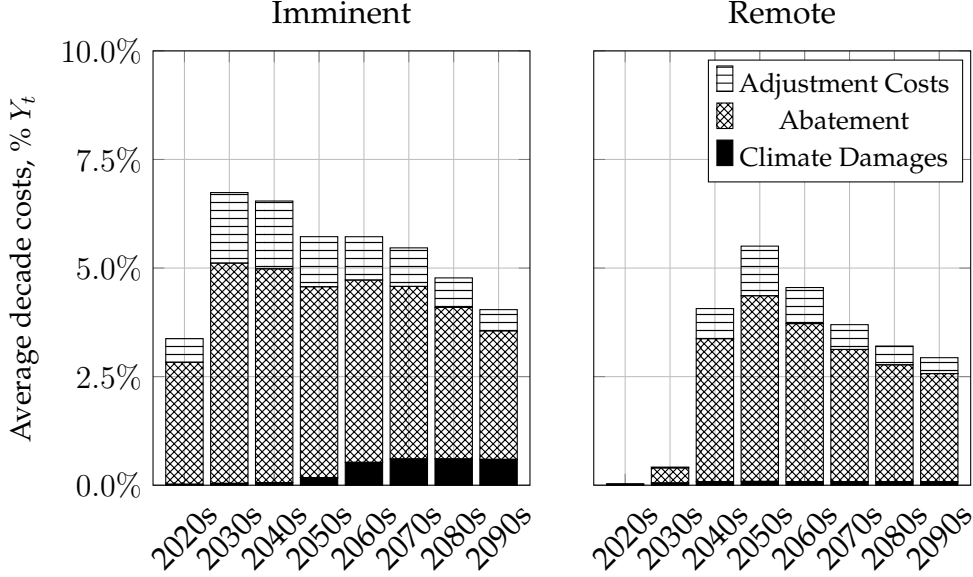

Figure 14: Costs in the median scenario as a fraction of output Y_t, broken down in adjustment costs, abatement and climate damages.

In case of an imminent tipping point (left panel), optimal abatement costs quickly ■ build up over the next two decades to around 5% of output before stabilising at 4% of output. Because abatement occurs quickly, society incurs in large adjustment costs of up to 2% of output, which are then absorbed over time. Despite these efforts, climate damages stabilise at around 1% of output. In case of a remote tipping point, the planner can scale abatement expenditures more slowly, thereby incurring in moderate adjustment costs and benefiting from improved technology. In both cases, the cost of the abatement required to stabilise the climate shrinks thanks to technological improvement ω_t (25), while climate damages are persistent as tipping points are irreversible.

The costs do not give the full picture, as the planner has preferences over consumption, given by the Epstein-Zin aggregator (31). To give estimates on the costs of tipping points under optimal policies, one needs to focus on the net present values, which satisfy (30) at time $t = 0$. Denote the net present value by $\overline{V}_0$, when the tipping point is remote, and $\underline{V}_0$, when the tipping point is

imminent. These two values can be translated into dollars by computing the corresponding certainty equivalence, that is the amount of constant and certain yearly output that yields the same net present value (more details on the calculation are given in Appendix B). This quantity internalises all future climate damages and output growth, and their respective uncertainties. In case of a remote tipping point, the certainty equivalent $\overline{CE}$ is 54.83 trillionUS\$/year (72.33% current output), while in case of an imminent tipping point, the certainty equivalent $\underline{CE}$ is 52.95 trillionUS\$/year (69.86% times current output). Hence, the cost of the tipping point being triggered at one degree lower, at $T^c = 1.5°$ rather than $T^c = 2.5°$, is 1.87 trillionUS\$/year or 2.47% of current output Y_0. Both certainty equivalents are significantly lower than

5 The Cost of Tipping Points Uncertainty

The previous section discussed the optimal policies of a planner that knows whether the tipping point is imminent or remote. Yet, tipping points are unpredictable. This section gives an upper bound on the cost of this unpredictability. To do so, I consider two extreme scenario. First, I consider a "wishful thinker" planner, denoted w, who erroneously assumes the tipping point to be remote, while it is in fact imminent. Once the climate feedback kicks in, the planner detects the tipping point and switches to the optimal abatement strategy. In other words, letting

$$\tau := \inf_t \{T_t \geq T^c\} \tag{32}$$

be the time at which the feedback effects kick-in, the abatement strategy employed by w is given by

$$\alpha_t^w := \begin{cases} \overline{\alpha}_t & \text{if } t < \tau, \\ \underline{\alpha}_t & \text{if } t \geq \tau. \end{cases} \tag{33}$$

Second, I consider a "prudent", denoted p, who erroneously assumes the tipping point to be imminent, while it is in fact remote. Again, in case the feedback

loop is triggered, the planner switches to the optimal strategy, such that

$$
\alpha_t^p := \begin{cases} \underline{\alpha}_t & \text{if } t < \tau, \\ \overline{\alpha}_t & \text{if } t \geq \tau. \end{cases} \tag{34}
$$

Table 1 summarises the possible tipping points and the strategies employed before the climate feedback are triggered, $t < \tau$. The tipping point can either be remote or imminent and each has an optimal policies, discussed in the previous section. If the tipping point is imminent, yet the planner behaves as if it is remote, we denote that by "wishful thinking" strategy w. If the tipping point is remote, yet the planner behaves as if it is imminent, we denote that by "prudent" strategy p.

		Tipping Point	
		Imminent	Remote
Policies	$\underline{\alpha}$	Optimal	Prudent p
	$\overline{\alpha}$	Wishful thinker w	Optimal

Table 1: Strategies used before tipping $t < \tau$ for the four scenarios. After tipping $t \geq \tau$ optimal strategies are used in all scenarios.

The wishful thinker planner w incurs in the maximal climate damages. The prudent planner p incurs in the maximal abatement and adjustment costs. Hence, the costliest of the two incorrect strategies is an upper bound to the cost of the tipping point.

Focusing first on the wishful thinker w, Figure 15 shows the path of the abated fraction of emissions ε_t (left panel) and the resulting temperature T_t (right panel) whenever α^w (33) is used in face of an imminent tipping point.
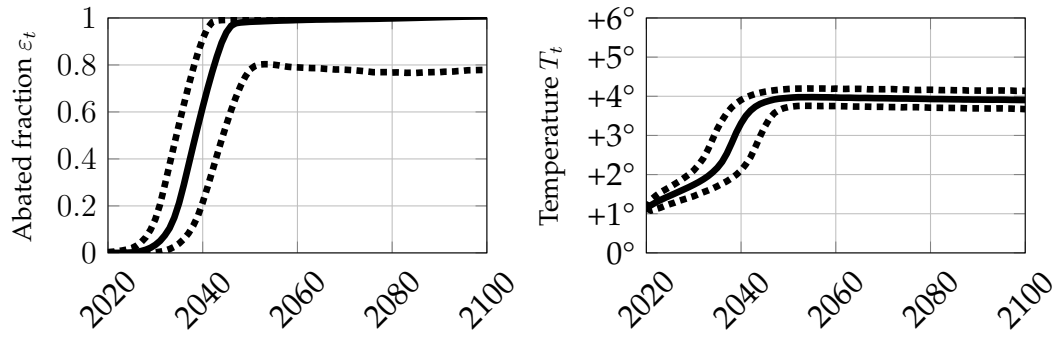
Figure 15: Median and 95% simulation intervals of the abated fraction of emissions ε_t (left panel) and the resulting the temperature T_t (right panel). Calculated from 10000 simulations using policy (33)

In the first decade, the planner erroneously believes the tipping point to be remote, and hence postpones abatement efforts, as the median $\varepsilon_t \approx 0$ for $t <$ 2030. Once the climate feedback kicks in, the planner "slams the break" and quickly ramps up abatement, achieving net-zero in the 2040s, in most cases. Despite the quick abatement rump-up, by 2050 the climate has tipped and is hence in a high temperature regime with 95% probability. When compared to the optimal abatement path under an imminent tipping point (left column of Figure 13), the abatement path path w clearly incurs in much larger climate damages, as the climate tips sooner and with large probability, and in larger adjustment costs, as abatement measures need to be ramped up more quickly. Figure 16 shows a breakdown of the cost incurred by the wishful thinker w.
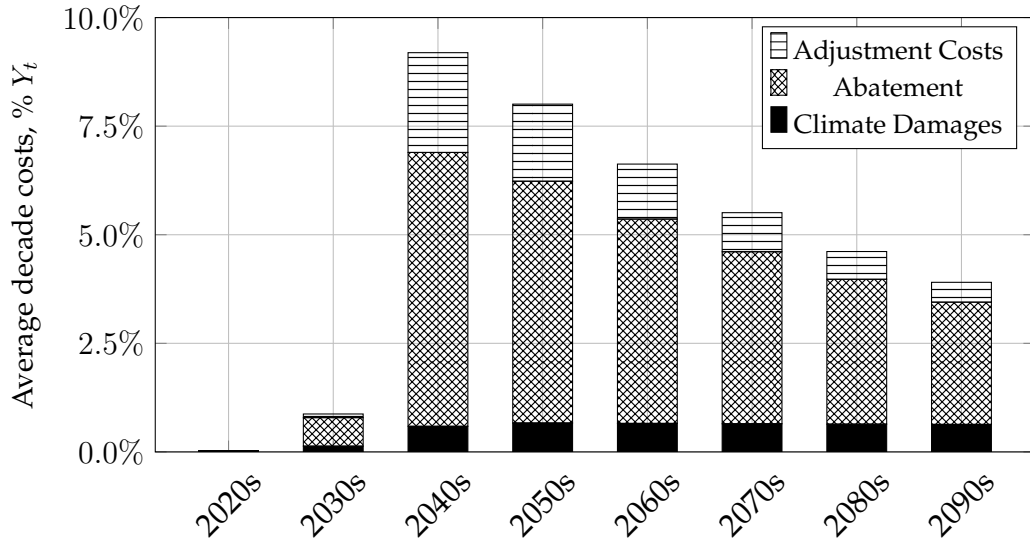
Figure 16: Costs in the median scenario of a wishful thinker w planner as a fraction of output Y_t, broken down in adjustment costs, abatement and climate damages.

In the first two decades, the planner implements little abatement measures. Yet, in the 2040s as positive climate feedbacks kick in, abatement expenditures rump up quickly. Rapidly ramping up abatement incurs in large adjustment costs.

A similar experiment can be done for the p planner. As above, Figure 17 displays the path of the abated fraction of emissions ε_t (left panel) and temperature T_t (right panel) resulting from abatement α^p (34) whenever the tipping point is remote.
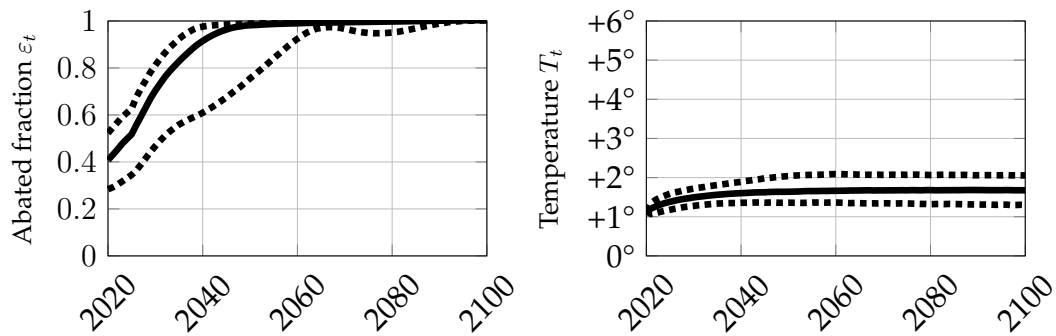

Figure 17: Median and 95% simulation intervals of the abated fraction of emissions ε_t (left panel) and the resulting the temperature T_t (right panel). Calculated from 10000 simulations using policy (34)

The prudent planner fully abates emissions already be the early 2040s and quickly stabilises temperature at around $2.5°$. Figure 18 breaks down the cost
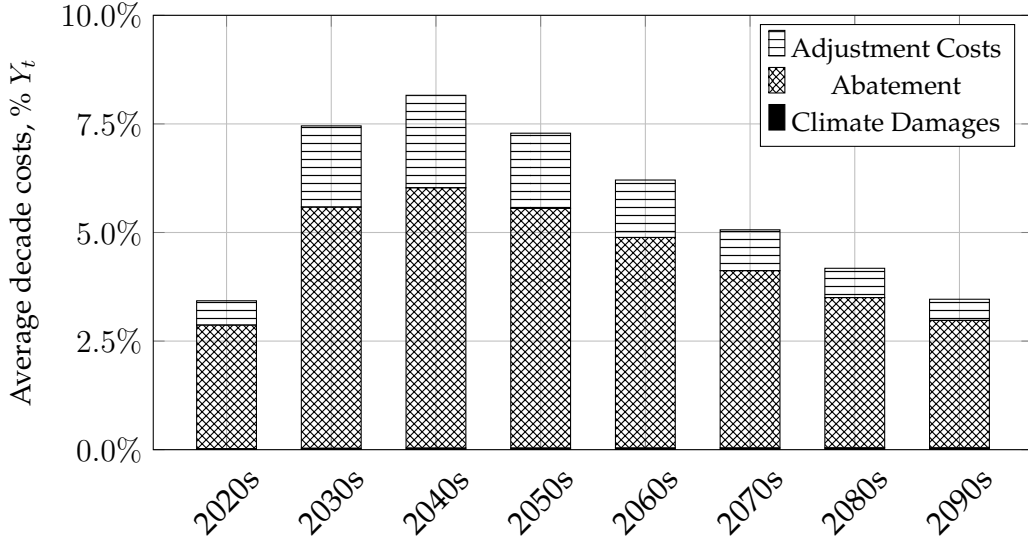
incurred by the prudent p planner.

Figure 18: Costs in the median scenario of a prudent p planner as a fraction of output Y_t, broken down in adjustment costs, abatement and climate damages.

This strategy incurs in large abatement and adjustment costs.

The breakdowns presented here (Figures 16 and 18) give upper bounds on the climate damages (w) and abatement cost (p). These are just nominal costs, that do reflect climate and economic risk and do not internalise societal preference. Hence, as in the optimal scenario presented in the previous section, I compute certainty equivalents CE^w and CE^p, in trillionUS\$/year, for the wishful thinker and prudent case respectively (more detail on how they are computed is given in Appendix B). These are summarised in Table 2.

		Tipping Point	
		Imminent	Remote
Policies	$\underline{\alpha}$	$\underline{CE} = 52.95\ (69.86\%)$	$CE^p = 29.92\ (39.48\%)$
	$\overline{\alpha}$	$CE^w = 26.7\ (35.23\%)$	$\overline{CE} = 54.83\ (72.33\%)$

Table 2: Certainty equivalents for the four scenarios in trillionUS\$/year. In brackets, the certainty equivalent is expressed as a percentage of current output Y_0.

The Table has the same structure as Table 1. Each cell contains the certainty equivalent of the corresponding scenario, in trillionUS\$/year and as a percent-

age of current output Y_0. These quantities allow to bound the cost of the tipping point. On the one hand, a prudent strategy p, in which society acts very rapidly to abate emissions under the assumption that a tipping point is imminent, incurs in suboptimal abatement and adjustment costs. These costs can be as high as $\overline{CE} - CE^p = 24.9$ trillionUS\$/year or 32.86% of current output. On the other hand, a wishful thinker strategy w, in which society delays abatement assuming that the tipping point is remote, incurs large and permanent climate damages. This can have costs up to $\underline{CE} - CE^w = 26.25$ trillionUS\$/year or 34.63% of current output.

The implications of the estimation are twofold. First, the cost of uncertainty of tipping points, which results in the inability of society to implement optimal strategies, can be as large as 26.25 trillionUS\$/year, which is more than a third of current world output. These large costs reflect the crucial role tipping points play when trying to deal with climate change: if they can be foreseen they are easily avoided; if they are ignored they can be catastrophic. Second, in the face of uncertainty, it is better to tread carefully, as prudence, however costly, is cheaper then wishful thinking.

6 Conclusion

References

Ackerman, Frank, Elizabeth A. Stanton, and Ramón Bueno. 2013. "Epstein–Zin Utility in DICE: Is Risk Aversion Irrelevant to Climate Policy?" *Environmental and Resource Economics*, 56(1): 73–84. 45

Armstrong McKay, David I., Arie Staal, Jesse F. Abrams, Ricarda Winkelmann, Boris Sakschewski, Sina Loriani, Ingo Fetzer, Sarah E. Cornell, Johan Rockström, and Timothy M. Lenton. 2022. "Exceeding 1.5°C Global Warming Could Trigger Multiple Climate Tipping Points." *Science*, 377(6611): eabn7950. 2, 5

Ashwin, Peter, Sebastian Wieczorek, Renato Vitolo, and Peter Cox. 2012. "Tipping Points in Open Systems: Bifurcation, Noise-Induced and Rate-Dependent Examples in the Climate System." *Philosophical Transactions of the Royal Society A: Mathematical, Physical and Engineering Sciences*, 370(1962): 1166–1184. 13

Baker, Erin, Leon Clarke, and Ekundayo Shittu. 2008. "Technical Change and the Marginal Cost of Abatement." *Energy Economics*, 30(6): 2799–2816. 21

Barro, Robert J. 2009. "Rare Disasters, Asset Prices, and Welfare Costs." *American Economic Review*, 99(1): 243–264. 4, 18

Ben-Yami, Maya, Andreas Morr, Sebastian Bathiany, and Niklas Boers. 2024. "Uncertainties Too Large to Predict Tipping Times of Major Earth System Components from Historical Data." *Science Advances*, 10(31): eadl4841. 2, 9, 13

Bierkens, Joris, Paul Fearnhead, and Gareth Roberts. 2019. "The Zig-Zag Process and Super-Efficient Sampling for Bayesian Analysis of Big Data." *The Annals of Statistics*, 47(3). 5, 44

Boulton, Chris A., Lesley C. Allison, and Timothy M. Lenton. 2014. "Early Warning Signals of Atlantic Meridional Overturning Circulation Collapse in a Fully Coupled Climate Model." *Nature Communications*, 5(1): 5752–5752. 13

Cai, Yongyang, Timothy M. Lenton, and Thomas S. Lontzek. 2016. "Risk of Multiple Interacting Tipping Points Should Encourage Rapid CO2 Emission Reduction." *Nature Climate Change*, 6(5): 520–525. 4

Crost, Benjamin, and Christian P. Traeger. 2013. "Optimal Climate Policy: Uncertainty versus Monte Carlo." *Economics Letters*, 120(3): 552–558. 45

Dell, Melissa, Benjamin F Jones, and Benjamin A Olken. 2009. "Temperature and Income: Reconciling New Cross-Sectional and Panel Estimates." *American Economic Review*, 99(2): 198–204. 19

Dell, Melissa, Benjamin F Jones, and Benjamin A Olken. 2012. "Temperature Shocks and Economic Growth: Evidence from the Last Half Century." *American Economic Journal: Macroeconomics*, 4(3): 66–95. 19

Dietz, Simon, and Bruno Lanz. 2019. "Growth and Adaptation to Climate Change in the Long Run." IRENE Institute of Economic Research IRENE Working Papers 19-09. 19

Dietz, Simon, and Frank Venmans. 2019. "Cumulative Carbon Emissions and Economic Policy: In Search of General Principles." *Journal of Environmental Economics and Management*, 96: 108–129. 21

Dietz, Simon, Frederick Van Der Ploeg, Armon Rezai, and Frank Venmans. 2020. "Are Economists Getting Climate Dynamics Right and Does It Matter?" *SSRN Electronic Journal*. 4

Ditlevsen, Peter D., and Sigfus J. Johnsen. 2010. "Tipping Points: Early Warning and Wishful Thinking." *Geophysical Research Letters*, 37(19): 2010GL044486. 13

Duffie, Darrell, and Larry G. Epstein. 1992. "Asset Pricing with Stochastic Differential Utility." *Review of Financial Studies*, 5(3): 411–436. 23

Epstein, Larry G., and Stanley E. Zin. 1989. "Substitution, Risk Aversion, and the Temporal Behavior of Consumption and Asset Returns: A Theoretical Framework." *Econometrica*, 57(4): 937. 43

Ghil, Michael, and Stephen Childress. 2012. *Topics in Geophysical Fluid Dynamics: Atmospheric Dynamics, Dynamo Theory, and Climate Dynamics.* Vol. 60, Springer Science & Business Media. 12

Greiner, Alfred, and Willi Semmler. 2005. "Economic Growth and Global Warming: A Model of Multiple Equilibria and Thresholds." *Journal of Economic Behavior & Organization*, 57(4): 430–447. 5

Hambel, Christoph, Holger Kraft, and Eduardo Schwartz. 2021. "Optimal Carbon Abatement in a Stochastic Equilibrium Model with Climate Change." *European Economic Review*, 132: 103642. 4, 5, 10, 17, 18, 20, 23, 40, 47

IPCC. 2023. *Climate Change 2021 – The Physical Science Basis: Working Group I Contribution to the Sixth Assessment Report of the Intergovernmental Panel on Climate Change.* . 1 ed., Cambridge University Press. 14, 18, 21

Kamien, Morton I., and Nancy L. Schwartz. 1971. "Sufficient Conditions in Optimal Control Theory." *Journal of Economic Theory*, 3(2): 207–214. 4

Kriegler, Elmar, Nico Bauer, Alexander Popp, Florian Humpenöder, Marian Leimbach, Jessica Strefler, Lavinia Baumstark, Benjamin Leon Bodirsky, Jérôme Hilaire, David Klein, Ioanna Mouratiadou, Isabelle Weindl, Christoph Bertram, Jan-Philipp Dietrich, Gunnar Luderer, Michaja Pehl, Robert Pietzcker, Franziska Piontek, Hermann Lotze-Campen, Anne Biewald, Markus Bonsch, Anastasis Giannousakis, Ulrich Kreidenweis, Christoph Müller, Susanne Rolinski, Anselm Schultes, Jana Schwanitz, Miodrag Stevanovic, Katherine Calvin, Johannes Emmerling, Shinichiro Fujimori, and Ottmar Edenhofer. 2017. "Fossil-Fueled Development (SSP5):

An Energy and Resource Intensive Scenario for the 21st Century." *Global Environmental Change*, 42: 297–315. 11

Kuik, Onno, Luke Brander, and Richard S.J. Tol. 2009. "Marginal Abatement Costs of Greenhouse Gas Emissions: A Meta-Analysis." *Energy Policy*, 37(4): 1395–1403. 21

Kushner, Harold J., and Paul Dupuis. 2001. *Numerical Methods for Stochastic Control Problems in Continuous Time.* Vol. 24 of *Stochastic Modelling and Applied Probability*, New York, NY:Springer New York. 5, 42, 43

Lemoine, Derek, and Christian P. Traeger. 2016. "Ambiguous Tipping Points." *Journal of Economic Behavior & Organization*, 132: 5–18. 4, 17

Lemoine, Derek, and Christian Traeger. 2014. "Watch Your Step: Optimal Policy in a Tipping Climate." *American Economic Journal: Economic Policy*, 6(1): 137–166. 4

Le Quéré, Corinne, Christian Rödenbeck, Erik T. Buitenhuis, Thomas J. Conway, Ray Langenfelds, Antony Gomez, Casper Labuschagne, Michel Ramonet, Takakiyo Nakazawa, Nicolas Metzl, Nathan Gillett, and Martin Heimann. 2007. "Saturation of the Southern Ocean CO2 Sink Due to Recent Climate Change." *Science*, 316(5832): 1735–1738. 11

Li, Chuan-Zhong, Anne-Sophie Crépin, and Therese Lindahl. 2024. "The Economics of Tipping Points: Some Recent Modeling and Experimental Advances." *International Review of Environmental and Resource Economics*, 18(4): 385–442. 4, 17

Lontzek, Thomas S., Yongyang Cai, Kenneth L. Judd, and Timothy M. Lenton. 2015. "Stochastic Integrated Assessment of Climate Tipping Points Indicates the Need for Strict Climate Policy." *Nature Climate Change*, 5(5): 441–444. 4, 45

Mäler, Karl-Göran, Anastasios Xepapadeas, and Aart de Zeeuw. 2003. "The Economics of Shallow Lakes." *Environmental and Resource Economics,* 26(4): 603–624. 5

McGuffie, Kendal, and Ann Henderson-Sellers. 2014. *The Climate Modelling Primer. .* 4. ed ed., Chicester:Wiley Blackwell. 4, 13, 14

Mogensen, Patrick Kofod, and Asbjørn Nilsen Riseth. 2018. "Optim: A Mathematical Optimization Package for Julia." *Journal of Open Source Software,* 3(24): 615. 44

Nævdal, Eric, and Michael Oppenheimer. 2007. "The Economics of the Thermohaline Circulation—A Problem with Multiple Thresholds of Unknown Locations." *Resource and Energy Economics,* 29(4): 262–283. 4

Nordhaus, William. 2019. "Economics of the Disintegration of the Greenland Ice Sheet." *Proceedings of the National Academy of Sciences,* 116(25): 12261–12269. 5

Nordhaus, William D. 1992. "An Optimal Transition Path for Controlling Greenhouse Gases." *Science,* 258(5086): 1315–1319. 20, 21

Nordhaus, William D. 2014. "Estimates of the Social Cost of Carbon: Concepts and Results from the DICE-2013R Model and Alternative Approaches." *Journal of the Association of Environmental and Resource Economists,* 1(1): 273–312. 45

Nordhaus, William D. 2017. "Revisiting the Social Cost of Carbon." *Proceedings of the National Academy of Sciences of the United States of America,* 114(7): 1518–1523. 21

Pindyck, Robert S, and Neng Wang. 2013. "The Economic and Policy Consequences of Catastrophes." *American Economic Journal: Economic Policy,* 5(4): 306–339. 4, 18, 23

Rackauckas, Christopher, and Qing Nie. 2017. "Adaptive Methods for Stochastic Differential Equations via Natural Embeddings and Rejection Sampling with Memory." *Discrete and continuous dynamical systems. Series B*, 22(7): 2731. 44

Seaver Wang, A. Foster, E. A. Lenz, J. Kessler, J. Stroeve, L. Anderson, M. Turetsky, R. Betts, Sijia Zou, W. Liu, W. Boos, and Z. Hausfather. 2023. "Mechanisms and Impacts of Earth System Tipping Elements." *Reviews of Geophysics*. 2, 5, 13

Shi, Hao, Hanqin Tian, Naiqing Pan, Christopher P. O. Reyer, Philippe Ciais, Jinfeng Chang, Matthew Forrest, Katja Frieler, Bojie Fu, Anne Gädeke, Thomas Hickler, Akihiko Ito, Sebastian Ostberg, Shufen Pan, Miodrag Stevanović, and Jia Yang. 2021. "Saturation of Global Terrestrial Carbon Sink Under a High Warming Scenario." *Global Biogeochemical Cycles*, 35(10): e2020GB006800. 11

Skiba, A. K. 1978. "Optimal Growth with a Convex-Concave Production Function." *Econometrica*, 46(3): 527. 5

Smith, Christopher J., Piers M. Forster, Myles Allen, Nicholas Leach, Richard J. Millar, Giovanni A. Passerello, and Leighton A. Regayre. 2017. "FAIR v1.1: A Simple Emissions-Based Impulse Response and Carbon Cycle Model." 5

Tsur, Yacov, and Amos Zemel. 1996. "Accounting for Global Warming Risks: Resource Management under Event Uncertainty." *Journal of Economic Dynamics and Control*, 20(6-7): 1289–1305. 4

Van den Bremer, Ton S., and Frederick Van der Ploeg. 2021. "The Risk-Adjusted Carbon Price." *American Economic Review*, 111(9): 2782–2810. 4

Van Der Ploeg, Frederick, and Aart De Zeeuw. 2018. "Climate Tipping and Economic Growth: Precautionary Capital and the Price of Carbon." *Journal of the European Economic Association*, 16(5): 1577–1617. 4, 17

Van Westen, René M., Michael Kliphuis, and Henk A. Dijkstra. 2024. "Physics-Based Early Warning Signal Shows That AMOC Is on Tipping Course." *Science Advances*, 10(6): eadk1189. 13

Wagener, F. 2013. "Regime Shifts: Early Warnings." In *Encyclopedia of Energy, Natural Resource, and Environmental Economics*. 349–359. Elsevier. 5, 14

Wagener, Florian. 2015. "Economics of Environmental Regime Shifts." In *The Oxford Handbook of the Macroeconomics of Global Warming*. , ed. Lucas Bernard and Willi Semmler, 0. Oxford University Press. 5

Weitzman, Martin L. 2012. "GHG Targets as Insurance against Catastrophic Climate Damages." *Journal of Public Economic Theory*, 14(2): 221–244. 19, 20

Weitzman, Martin L. 2014. "Fat Tails and the Social Cost of Carbon." *American Economic Review*, 104(5): 544–546. 18

A   Solution to Maximisation

This appendix deals with the solution of the maximisation problem (30).

A.1   Simplifying Assumptions on the Decay Rate of Carbon

To reduce the state space, following Hambel, Kraft and Schwartz (2021), I make an assumption on the decay rate of carbon. The calibrated carbon decay δ_m, as a function of the carbon stored in sinks N_t, is illustrated in Figure 19. The calibration assumes a functional form

$$\delta_m(N_t) = a_\delta e^{-\left(\frac{N_t - c_\delta}{b_\delta}\right)^2}, \tag{35}$$

for parameters $a_\delta, b_\delta, c_\delta$.
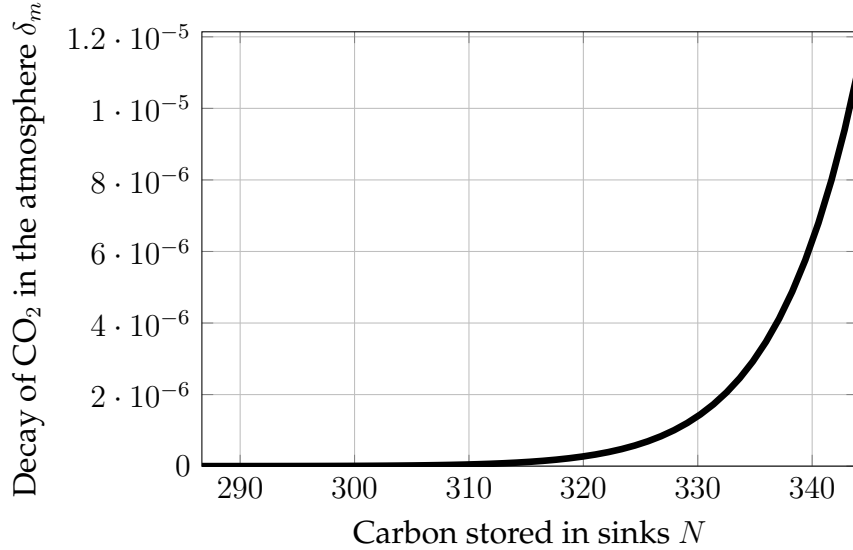
Figure 19: Estimated decay of carbon δ_m as a function of the carbon stored in sinks N_t.

I assume that the amount of carbon sinks present in the atmosphere is a constant fraction of the concentration in the atmosphere, $N_t = \frac{N_0}{M_0} M_t$. Abusing notation, I henceforth write $\delta_m(M_t)$ for the decay rate. Using this setup, under a business-as-usual emission scenario, the decay of carbon follows the path in Figure 20.
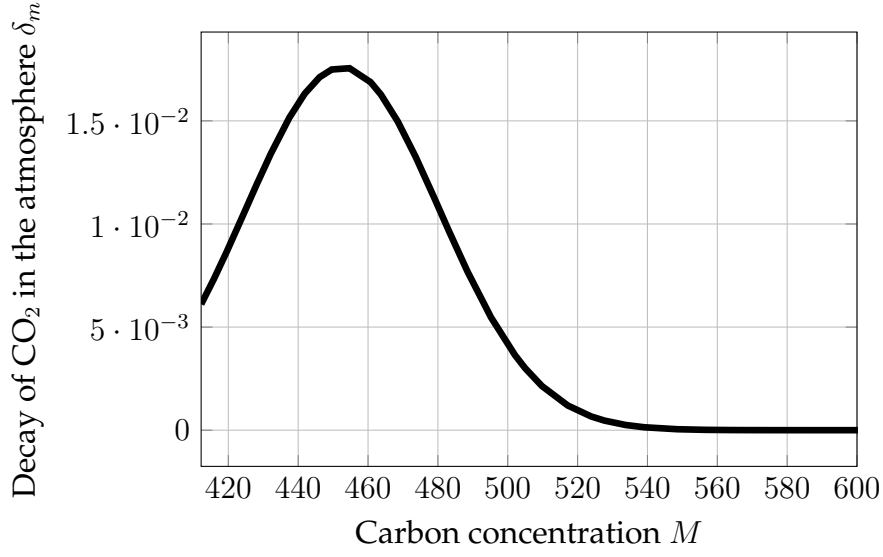
Figure 20: Estimated decay of carbon δ_m under the business as usual emission scenario M^b. Each marker is the decay after every decade.

A.2 Hamilton-Jacobi-Bellman equation

Using the assumption from Appendix A.1, the value function V at time t depends only on temperature T_t, log-carbon concentration m_t and output Y_t. This satisfies the Hamilton-Jacobi-Bellman equation

$$
\begin{aligned}
-\partial_t V = \sup_{\chi,\alpha} \; & f(\chi Y, V) + \partial_m V \, (\gamma_t^b - \alpha) + \partial_m^2 V \, \frac{\sigma_m^2}{2} \\
& + \partial_Y V (\varrho + \phi(\chi) - d(T) - \beta_t(\varepsilon(\alpha))) + \partial_k^2 V \, \frac{\sigma_Y^2}{2} \\
& + \partial_T V \, \frac{r(T) + g(m)}{\epsilon} + \partial_T^2 V \, \frac{(\sigma_T/\epsilon)^2}{2}.
\end{aligned}
\tag{36}
$$

It is easy to check that the ansatz

$$
V_t(T, m, Y) = \frac{Y^{1-\theta}}{1-\theta} F_t(T, m)
\tag{37}
$$

satisfies (36).

A.3 Approximating Markov Chain

The Hamilton-Jacobi-Bellman equation (36) is solved for F by adapting the method proposed in Kushner and Dupuis (2001). The idea is to discretise the state space of T and m and compute time dependent intervals $\Delta t(T, m)$. Then, constructing a Markov chain $\mathcal{M}$ over the discretised space, parametrised by some small step size h. Then we compute a discretised value function F^h with the property that $F^h \to F$ as $h \to 0$.

Given an h, construct a grid

$$\Omega_h = \{0, h, 2h, \ldots, 1-h, 1\}^2, \tag{38}$$

over the unit cube. This grid covers a suitable subset of the state space

$$\mathcal{X} := [T^p, T^p + \Delta T] \times [m^p, m^p + \Delta m] \tag{39}$$

where Δm is chosen such that $T^p + \Delta T$ is stable at $m^p + \Delta m$.

Using the ansatz (37) we can define a discrete value function F_t^h over the grid such that $F_t^h \to F_t$ as $h \to 0$ over χ, that is

$$
\begin{aligned}
F_t^h(T_t, m_t) = \min_{\chi, \alpha} \Bigg(& \left(1 - e^{-\rho \Delta t}\right) \chi^{1 - \frac{1}{\psi}} + \\
& e^{-\rho \Delta t} \left(\delta_y(\chi) \, \mathbb{E}_{t, \mathcal{M}(\alpha)} F_{t+\Delta t}^h(T_{t+\Delta t}, m_{t+\Delta t})\right)^{\frac{1 - \frac{1}{\psi}}{1 - \theta}} \Bigg)^{\frac{1 - \theta}{1 - \frac{1}{\psi}}}
\end{aligned}
\tag{40}
$$

where

$$
\begin{aligned}
\delta_y(\chi) &:= \mathbb{E}_t \left[\left(\frac{Y_{t+\Delta t}}{Y_t}\right)^{1-\theta} \right] \\
&= 1 + \Delta t (1 - \theta) \left(\varrho + \phi(\chi) - d(T_t) - \frac{\theta}{2}\sigma_k^2 \right) + \mathbb{E}_t \left[o(\Delta t^{\frac{3}{2}}) \right].
\end{aligned}
\tag{41}
$$

and $\mathbb{E}_{t, \mathcal{M}(\alpha)}$ is the expectation with respect to the Markov chain $\mathcal{M}(\alpha)$ over the grid. This can be constructed, given a step size h, as follows. Introduce the

normalising factor

$$Q_t(T, m, \alpha) := \left(\frac{\sigma_T}{\epsilon \Delta T}\right)^2 + \left(\frac{\sigma_m}{\Delta m}\right)^2 + h\left|\frac{r(T) + g(m)}{\epsilon \Delta T}\right| + h\left|\frac{\gamma_t^b - \alpha}{\Delta m}\right|. \tag{42}$$

Then the probabilities of moving from a point (T, m) of the grid to an adjacent point are given by

$$p(T \pm h\Delta T, m \mid T, m) \propto \frac{1}{2}\left(\frac{\sigma_T}{\epsilon \Delta T}\right)^2 + h\left(\frac{r(T) + g(m)}{\epsilon \Delta T}\right)^{\pm} \quad \text{and} \tag{43}$$

$$p(T, m \pm h\Delta m \mid T, m) \propto \frac{1}{2}\left(\frac{\sigma_m}{\Delta m}\right)^2 + h\left(\frac{\gamma_t^b - \alpha}{\Delta m}\right)^{\pm} \tag{44}$$

where $(\cdot)^+ := \max\{\cdot, 0\}$ and $(\cdot)^- := -\min\{\cdot, 0\}$. One can readily check that this is a well defined probability measure. Finally, the time step is given by

$$\Delta t = h^2/Q_t(T, m, \alpha), \tag{45}$$

which satisfies $\Delta t \to 0$ as $h \to 0$.

Then, as the aggregator used in (40) converges to f (31) (Epstein and Zin, 1989), the chain described here satisfies the convergence properties outlined in Kushner and Dupuis (2001), we have $F_t^h \to F_t$ as $h \to 0$.

The Markov chain defined above allows to derive $F_t^h(T_t, m_t)$ from the subsequent $F_{t+\Delta t}^h(T_{t+\Delta t}, m_{t+\Delta t})$. This requires a terminal condition $\bar{F}^h(T_\tau, m_\tau) := F_\tau^h(T_\tau, m_\tau)$. To derive this, assume that at some point in a far future $\tau \gg 0$, the abatement is free and all emissions are abated, $\gamma^b = \alpha$, such that $\mathrm{d}m = \sigma_m \,\mathrm{d}W_m$. Then we construct an equivalent, control independent, Markov chain $\bar{\mathcal{M}}$ as above for

$$\bar{F}^h(T_t, m_t) = \min_{\chi} \left(\left(1 - e^{-\rho\Delta t}\right) \chi^{1-\frac{1}{\psi}} + \right.$$
$$\left. e^{-\rho\Delta t} \left(\delta_y(\chi)\, \mathbb{E}_{t, \bar{\mathcal{M}}} \bar{F}^h(T_{t+\Delta t}, m_{t+\Delta t})\right)^{\frac{1-\frac{1}{\psi}}{1-\theta}} \right)^{\frac{1-\theta}{1-\frac{1}{\psi}}}. \tag{46}$$

This is now a fixed point equation for $\bar{F}$ which can be solved by value or policy

function iteration.

A.4 Parallelisation

When computing the backward recurrence (40), each grid point $X_i \in \mathcal{X}$ is assigned a different time step $\Delta t(X_i)$, which depends on the curvature of the drift at that state. To parallelise the computation, I leverage the ZigZag algorithm by Bierkens, Fearnhead and Roberts (2019). Given the value function F_t^h, for a step back $t - \min_i \Delta t(X_i)$, I construct a directed graph among grid points $\mathcal{X}$ where an edge $X_i \to X_j$ is drawn if there is a positive probability of transitioning from X_i to X_j under the Markov Chain $\mathcal{M}$. This allows to obtain, at each point in time t, sets of points $\mathcal{C}_t \subseteq \mathcal{X}$ which are independent and over which it is possible to parallelise. The parallelisation is then conducted on the Snellius, the national high performance computer of the Netherlands. The algorithm is written in the `Julia` programming language and relies on `Optim.jl` (Mogensen and Riseth, 2018) and `StochasticDifferentialEquations.jl` (Rackauckas and Nie, 2017).

B Certainty Equivalence

This appendix defines the certainty equivalence, which allows to translate net present values to monetary values in the context of our problem. Let $X_t :=$ (T_t, M_t, N_t, Y_t) be the state at time t and denote by $\overline{\mu}$ and $\underline{\mu}$ the drift functions of X_t under a remote and an imminent tipping point respectively. Such that, in case of remote tipping,

$$d\overline{X}_t = \overline{\mu}_t(X_t)\, dt + \Sigma\, dW_t \text{ where} \tag{47}$$

$$\Sigma := \operatorname{diag}(\sigma_T/\epsilon, \sigma_m, 0, \sigma_k) \tag{48}$$

and dW_t is a standard Wiener process. Under these dynamics, one can obtain the net present value in utils of the consumption stream $\overline{V}_0$ and $\underline{V}_0$ satisfying

equation (30). In a similar way one can compute the net present value of the consumption stream in utils of the wishful thinker (w) and prudent (p) policies as

$$V_0^i = \mathbb{E}_t \int_0^\infty f(Y_t \chi_t^i, V_t^i) \, \mathrm{d}t \tag{49}$$

with $i \in \{w, p\}$. For each $V \in \{\overline{V}, \underline{V}, V^w, V^p\}$, the corresponding certainty equivalent CE solves

$$V_0^i = f(CE, V_0^i). \tag{50}$$

C   Calibration and Parameters

This section summarises the parameters for the preferences, economy, and climate model and discusses the calibration strategy.

The following Table 3 illustrates the preferences parameters used throughout the paper. There is no consensus in the literature on preference parameters. In line with previous literature focusing on recursive preferences, I set relative risk aversion $\theta = 10$ (Ackerman, Stanton and Bueno, 2013; Crost and Traeger, 2013; Lontzek et al., 2015) and the time preference parameter $\rho = 1.5\%$ (Nordhaus, 2014). There is no consensus on whether the elasticity of intertemporal substitution ψ ought to be larger or smaller than unity, with the aforementioned papers using values $\psi \in [0.75, 1.5]$. In this paper, I use $\psi = 1.5$ for the benchmark model and test the robustness of the results to $\psi = 0.75$.

Preferences		
ρ	1.5%	Time preference
θ	10	Relative risk aversion
ψ	1.5	Elasticity of intertemporal substitution

Table 3

Table 4 summarises the parameters of the economy model.

Economy		
ω_0	11%	GDP loss required to fully abate today
ω_r	2.7%	Rate of abatement cost reduction
ϱ	0.9%	Growth of TFP
κ	6.32%	Adjustment costs of abatement technology
δ_k	0.0116	Initial depreciation rate of capital
ξ	0.00026	Coefficient of damage function
ν	3.25	Exponent of damage function
A_0	0.113	Initial TFP
Y_0	75.8	Initial GDP
σ_k	0.0162	Variance of GDP
τ	500	Steady state horizon

Table 4

Table 5 summarises the parameters of the climate model.

Climate		
T_0	288.56 [K]	Initial temperature
T^{p}	287.15 [K]	Pre-industrial temperature
M_0	410 [p.p.m.]	Initial carbon concentration
M^{p}	280 [p.p.m.]	Pre-industrial carbon concentration
N_0	286.65543 [p.p.m.]	Initial carbon in sinks
σ_T	1.5844	Volatility of temperature
S_0	342 [W / m²]	Mean solar radiation
ϵ	15.844 [J / m² K year]	Heat capacity of the ocean
η	$5.67e-8$	Stefan-Boltzmann constant
G_1	20.5 [W / m²]	Effect of CO_2 on radiation budget
G_0	150 [W / m²]	Pre-industrial GHG radiation budget

Table 5

Non-linearity		
ΔT	1.8 [K]	temperature inflection point
λ_1	31%	Initial radiation reflected
$\Delta \lambda$	.	.

D   Stochastic Tipping Benchmark Model

This appendix introduces a benchmark model with stochastic tipping. The stochastic tipping model is a widely used in the economic literature to approximate tipping points in the climate dynamics (e.g. Hambel, Kraft and Schwartz 2021). Comparing the model developed in this paper with the stochastic tipping model allows us to determine if and how the optimal abatement differ and, as a consequence, what the approximation misses.

To establish a meaningful benchmark, I will assume that the contribution of temperature to forcing (15) is given by

$$r_T^l(T_t) \coloneqq S_0(1 - \lambda_1) - \eta \sigma T_t^4. \tag{51}$$

This model has no tipping point as $\lambda(T_t) \equiv \lambda_1$. Stochastic tipping, as commonly modelled in the literature, is introduced as a jump process J_t with arrival rate $\pi(T_t)$ and intensity $\Theta(T_t)$, both increasing in temperature. Intuitively, as temperature rises, the risk of tipping $\pi(T_t)$ and the size of the temperature increase $\Theta(T_t)$ grow. Then temperature dynamics in the Stochastic Tipping model follow

$$\epsilon \, \mathrm{d}T_t = r^l(T_t) \, \mathrm{d}t + g(m) \, \mathrm{d}t + \sigma_T \, \mathrm{d}W_{s,t} + \Theta(T_t) \, \mathrm{d}J_t \tag{52}$$

where W_s is a Wiener process. Following Hambel, Kraft and Schwartz (2021),

the calibrated arrival rate and temperature increase are calibrated as

$$\pi(T_t) = -\frac{1}{4} + \frac{0.95}{1 + 2.8e^{-0.3325(T_t - T_t^{\mathrm{P}})}} \text{ and} \tag{53}$$

$$\Theta(T_t) = -0.0577 + 0.0568(T_t - T_t^{\mathrm{P}}) - 0.0029(T_t - T_t^{\mathrm{P}})^2. \tag{54}$$